

The aggregation process in tetraethoxysilane-derived sonogels as an analogy to the critical phenomenon

This article has been downloaded from IOPscience. Please scroll down to see the full text article.

2008 J. Phys.: Condens. Matter 20 255216

(<http://iopscience.iop.org/0953-8984/20/25/255216>)

View [the table of contents for this issue](#), or go to the [journal homepage](#) for more

Download details:

IP Address: 129.252.86.83

The article was downloaded on 29/05/2010 at 13:14

Please note that [terms and conditions apply](#).

The aggregation process in tetraethoxysilane-derived sonogels as an analogy to the critical phenomenon

D R Vollet, D A Donatti and A Ibañez Ruiz

Departamento de Física, IGCE, Unesp—Universidade Estadual Paulista, POB 178, CEP 13500-970 Rio Claro (SP), Brazil

E-mail: vollet@rc.unesp.br

Received 21 February 2008, in final form 19 April 2008

Published 21 May 2008

Online at stacks.iop.org/JPhysCM/20/255216

Abstract

The structural evolution in silica sols prepared from tetraethoxysilane (TEOS) sonohydrolysis was studied *in situ* using small-angle x-ray scattering (SAXS). The structure of the gelling system can be reasonably well described by a correlation function given by $\gamma(r) \sim (1/R^2)(1/r) \exp(-r/\xi)$, where ξ is the structure correlation length and R is a chain persistence length, as an analogy to the Ornstein–Zernike theory in describing critical phenomenon. This approach is also expected for the scattering from some linear and branched molecules as polydisperse coils of linear chains and random f -functional branched polycondensates. The characteristic length ξ grows following an approximate power law with time t as $\xi \sim t^1$ (with the exponent quite close to 1) while R remains undetermined but with a constant value, except at the beginning of the process in which the growth of ξ is slower and R increases by only about 15% with respect to the value of the initial sol. The structural evolution with time is compatible with an aggregation process by a phase separation by coarsening. The mechanism of growth seems to be faster than those typically observed for pure diffusion controlled cluster–cluster aggregation. This suggests that physical forces (hydrothermal forces) could be actuating together with diffusion in the gelling process of this system. The data apparently do not support a spinodal decomposition mechanism, at least when starting from the initial stable acid sol studied here.

1. Introduction

The structure and the kinetics of formation of alkoxyde-derived silica gels have been the object of several studies [1–8]. The overall sol–gel process of silicon alkoxydes deals with hydrolysis and polycondensation reactions of the precursors through a series of possible events that lead to the evolution of the gelling system from the initial homogeneous sol of silicon oligomers up to the final gel. The structure of the final gels depends upon the initial conditions of preparation and, in particular, strongly on the pH conditions for the hydrolysis and polycondensation. It is generally accepted that hydrolysis under acid conditions and excess of water leads to the formation of gels with structure that can be described as a mass fractal probably formed by clustering of branched polycondensates or linear chain coils.

The structural evolution of the gelling system has been discussed on the basis of chemical mechanisms, mainly at

the beginning of the process [7] and, more recently [6, 8], of physical restructuring which can take the form of a phase separation. The sol–gel transition which accompanies the formation of silica gels from hydrolysis of silicon alkoxydes has been thought of as an analogy to the critical phenomenon [9–13]. In this sense, there would be a correlation between the time evolution of the (irreversible) gelling system and the equilibrium temperature as the critical point is approached in the phase transition associated to the critical phenomenon [14].

In a previous work [5], using small-angle x-ray scattering (SAXS), we studied the kinetics of aggregation of tetraethoxysilane-(TEOS)-derived gelling systems prepared from solventless TEOS sonohydrolysis, in a two-step acid–base process. It was concluded, on the basis of a mass fractal approach, that the structural evolution associated to the gelling system can be described in terms of the evolution of small

clusters which are formed in the homogeneous stable sol in the acid step (pH = 2). The clusters seem to be lightly restructured on passing to the base step (pH = 4.5) and the structure evolves by means of an aggregation mechanism, in which the mass fractal dimension D is kept at an approximately constant value ($D \sim 2$), while the characteristic length of the mass fractal structure is increased up to the formation of a gel. The sol-gel structural evolution seems to be timescaling since the same picture is observed as the aggregation temperature is varied [5].

In this work, we realized that the structural evolution of a TEOS-derived gelling system prepared from sonohydrolysis of TEOS could be equally well described in terms of a very simple model on the basis of the Ornstein–Zernike theory [14] in an analogy to the phase transition in critical phenomena. This approach is also expected for the scattering from some linear and branched molecules as polydisperse coils of linear chains and random f -functional branched polycondensates [15]. The results and implications are discussed on the basis of this simple model.

2. Experimental procedure

TEOS, distilled and deionized water, and hydrochloric acid were used to prepare samples of about 76 ml of a TEOS–water–HCl reactant mixture with water/TEOS molar ratio equal to 6.5 and pH = 2.0. Hydrolysis of the mixture was promoted for 10 min under action of constant power ($\sim 0.7 \text{ W cm}^{-3}$) ultrasonic radiation. The hydrolysis is almost complete within 5 min under these experimental conditions [16]. Next, the sample was diluted in 28.6 ml of water and sonication was continued for more than 2 min for complete homogenization. The final water/TEOS molar ratio of the resulting sol was equal to 14.4, which is equivalent to a silica concentration of $\sim 2 \times 10^{-3} \text{ mol SiO}_2 \text{ cm}^{-3}$. This value corresponds to a volume fraction ϕ of silica approximately equal to 0.06. The sol was studied as obtained by SAXS. The pH of the resulting sol was adjusted to 4.5 by addition of NH_4OH and the time evolution of the SAXS intensity was measured ‘*in situ*’ at 60 °C. The sample was injected in a 1 mm thickness laminar space sealed with 10 μm -thickness Mylar sheets and placed in a special sample holder with temperature control.

The SAXS experiments were carried out using synchrotron radiation at LNLS (Campinas, Brazil) with a wavelength $\lambda = 0.1608 \text{ nm}$. The beam was monochromatized using a silicon monochromator and collimated by a set of slits defining a pinhole geometry. A one-dimensional position sensitive x-ray detector was used to record the SAXS intensity as a function of the modulus of the scattering vector $q = (4\pi/\lambda) \sin(\theta/2)$, where θ is the scattering angle, from $q_0 = 0.18 \text{ nm}^{-1}$ up to $q_m = 4.4 \text{ nm}^{-1}$ in intervals of $\Delta q = 3.36 \times 10^{-3} \text{ nm}^{-1}$. The data were corrected by the parasitic scattering and the sample attenuation and normalized by the beam intensity.

3. Results

Figure 1 shows the time evolution of the SAXS intensity $I(q)$ as measured ‘*in situ*’ for the gelling system at pH = 4.5 and

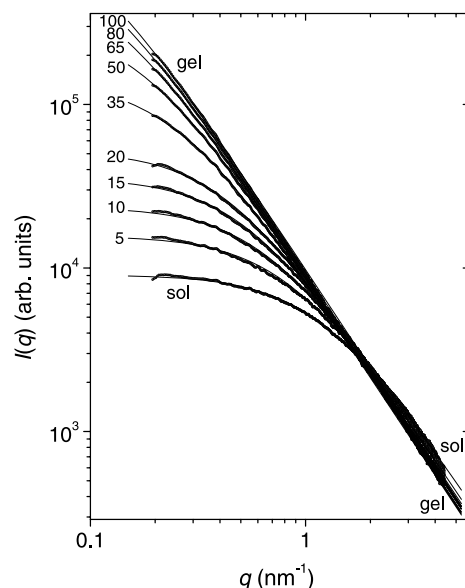


Figure 1. The time evolution of the SAXS intensity at 60 °C for the gelling system prepared from TEOS sonohydrolysis. Times are given in minutes. The solid lines are fittings of equation (1) to the experimental data, using a nonlinear least squares interaction routine (Levenberg–Marquardt algorithm).

60 °C. The data were compared with the SAXS intensity of the original stable sol at pH = 2. The sample associated with the last time of measurement was named ‘gel’ although the gel point could not be so easily defined in this system. All the curves follow approximately the relationship q^{-2} at some extension of the high q region and approximately a Gaussian curve at low- q . At the gel point, the intensity practically follows the relationship q^{-2} in almost all the range of q studied in the present work, except at very low- q . The dependence q^{-2} is expected to be produced from large subsections of polydisperse coils of linear chains or branched polycondensates of random f -functional elements [15, 17]. The low- q regime is produced by the finite size of such macromolecules or clusters.

A convenient description of both the regimes, at low- q and high- q , for the SAXS intensity can be made using the simple Burchard approach for polydisperse coils of linear chains or branched polycondensates of random f -functional elements [15]. That is the same relationship from the Ornstein–Zernike approximation in the description of the critical phenomenon [14] and can be cast as

$$I(q) = I(0)/(1 + \xi^2 q^2) \quad (1)$$

where ξ is the correlation length of the structure, a parameter which is proportional to the radius of gyration ($R_G = 3^{1/2}\xi$) of the macromolecule or cluster, and $I(0)$ accounts for the intensity at $q = 0$. From the Ornstein–Zernike approximation [14],

$$I(0) \sim \xi^2/R^2 \quad (2)$$

where R is called the Debye persistence length in the case of linear chains [17], but here we regard it as a phenomenological

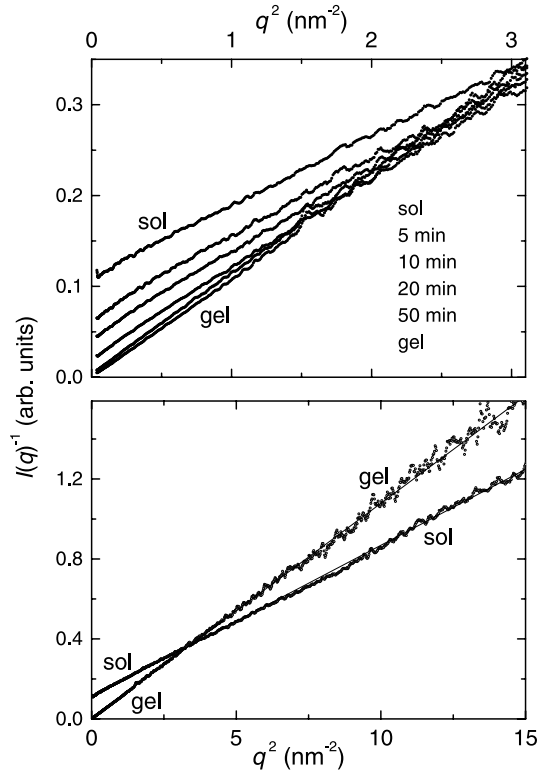


Figure 2. Zimm's plots showing the time evolution of the (irreversible) gelling system as an analogy with the critical point approaching the critical phenomena.

Table 1. Evolution of the structural parameters of the gelling system at 60 °C.

t (min)	$I(0)$ (arb. units)	ξ (nm)	R/R_{sol}
0 (sol)	0.91 ± 0.01	0.838 ± 0.008	1.00 ± 0.04
5	1.56 ± 0.02	1.19 ± 0.02	1.08 ± 0.04
10	2.36 ± 0.03	1.51 ± 0.02	1.12 ± 0.04
15	3.53 ± 0.03	1.90 ± 0.03	1.15 ± 0.04
20	5.21 ± 0.05	2.34 ± 0.03	1.17 ± 0.04
35	14.0 ± 0.1	4.02 ± 0.05	1.22 ± 0.04
50	31.4 ± 0.3	5.94 ± 0.07	1.20 ± 0.04
65	59.2 ± 0.5	8.07 ± 0.09	1.19 ± 0.04
80	91.4 ± 0.9	9.84 ± 0.09	1.17 ± 0.04
100 (gel)	124 ± 1	11.2 ± 0.1	1.14 ± 0.04

parameter since we have no way to determine it in absolute units of length. Equation (2) also holds for the scattering from a mass fractal cluster with characteristic length ξ (constant R) and mass fractal dimension $D = 2$ [18]. Figure 1 shows equation (1) fitting reasonably well to the experimental SAXS data. Table 1 shows the time dependence of the values fitted for $I(0)$ and ξ , and also for the relative variation R/R_{sol} of the persistence length R with respect to the value of the sol (R_{sol}). R/R_{sol} was determined from the relative variations of $I(0)$ and ξ through the relationship $R/R_{\text{sol}} = (\xi/\xi_{\text{sol}})[I(0)_{\text{sol}}/I(0)]^{1/2}$. $I(0)$ and ξ increase with time while R/R_{sol} is practically a constant value, after a rapid increase of about 15% at the beginning of the process.

Figure 2 shows the Zimm plots $I(q)^{-1}$ versus q^2 for the gelling system. The time evolution of the intercept $I(0)^{-1}$ in

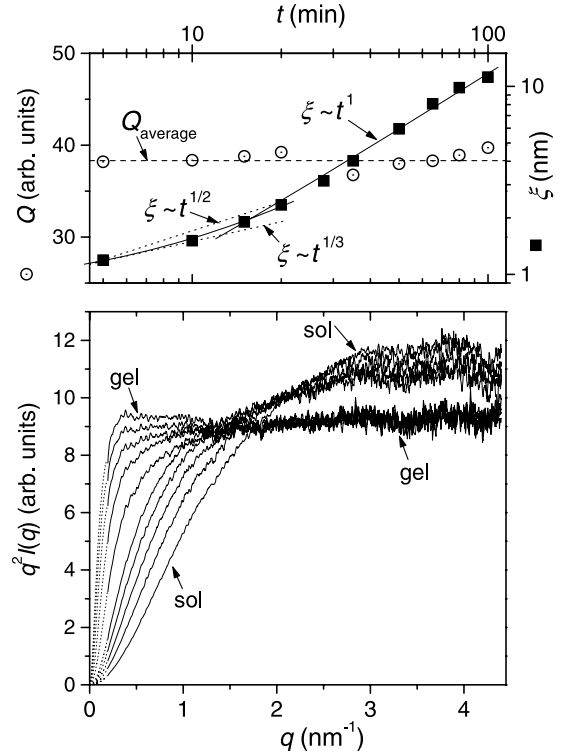


Figure 3. Bottom: Kratky's plots along the evolution of the gelling system. The dotted lines in the region $q < q_0$ are data extrapolated to $q = 0$ using the parameters $I(0)$ and ξ obtained from the fittings of equation (1). Top: time evolution of the invariant Q and of the structure characteristic length ξ .

the Zimm plots, going to zero as the gelling system approaches the gel point, is mainly associated with the increase of the correlation length ξ of the structure, while the minor variation in the slope of the Zimm plots is mainly associated with variations in the persistence length R .

Figure 3 (bottom) shows the Kratky plots $q^2 I(q)$ versus q for the gelling system. All the curves reach plateau values at some extension of the high- q region, as expected for the dependence $\sim q^{-2}$ found for the intensity there. The most striking feature of the particle scattering factors of the other branched models is the appearance of a maximum in the Kratky plots [15].

For a two-phase system of volume V , as is the case for this silica-liquid two-phase system in which the volume fractions of the phases are ϕ (silica) and $(1-\phi)$ (liquid), the SAXS intensity integrated over the reciprocal space q , a quantity usually called the Porod invariant, is given by

$$Q = \int_0^\infty q^2 I(q) dq = 2\pi^2 (\Delta\rho)^2 \phi(1-\phi)V \quad (3)$$

where $(\Delta\rho)$ is the difference in the electronic density of the phases. The integral Q is expected to be constant during structural transformations in which $(\Delta\rho)$ and the volume fractions ϕ and $(1-\phi)$ are kept constant. Q was evaluated numerically within the experimental range $q_0 \leq q \leq q_m$ and by extrapolation of $I(q)$ using equation (1) in the range $0 \leq q < q_0$. No extrapolation for $I(q)$ in the range $q > q_m$ has

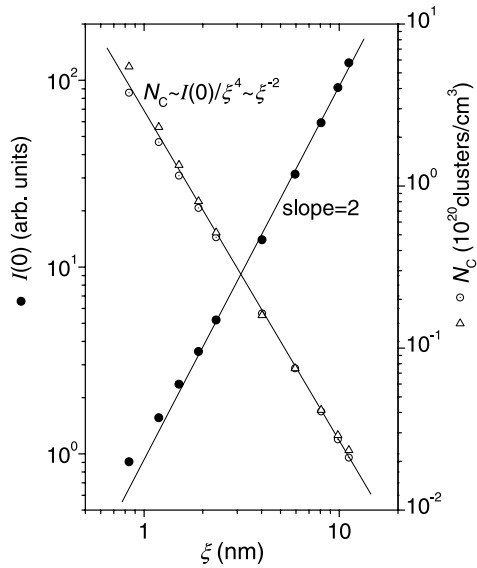


Figure 4. Left axis: the SAXS intensity $I(0)$ extrapolated to $q = 0$ following an approximate law $I(0) \sim \xi^2$. Right axis: the number of clusters per unit volume of the sample as evaluated from equation (4) (circles) and from equation (5) (triangles). The proportionality constant of equation (4) was adjusted to match equation (5) at $\xi = 5.9$ nm.

been assumed for evaluation of that contribution on the integral Q , so it has been neglected.

Figure 3 (top) shows that Q is practically a constant value during the stage studied in the present work. Then, the difference of the electronic density between the phases (particles and liquid matrix) and the volume fractions ϕ and $(1 - \phi)$ of the phases are approximately constant along the transformations accompanying the gelling system. Figure 3 (top) shows the time evolution of the characteristic length ξ along the gelling process. ξ increases approximately following a power law with time t as $\xi \sim t^1$ (with an exponent quite close to 1), after an initial period of about 15 min in which the increase of ξ with time is an ill-defined power law growth with exponent varying between 1/3 and 1/2 (figure 3). The $\xi \sim t^1$ growth of the present work is more rapid than that earlier $R_G \sim t^{1/2}$ observed by probing the radius of gyration directly from Guinier’s law instead of ξ from equation (1) [5]. It could be due to the fact that equation (1) seems to describe better the entire curve of SAXS in this system.

Figure 4 shows equation (2) describing well the relation between $I(0)$ and the correlation length ξ along the gelling process, except during that mentioned initial period of rapid increase of about 15% in the persistence length R . For a system of macromolecules in solution, the intensity $I(0)$ scattered at $q = 0$ is proportional to the mass concentration c_0 and to the molecular weight M of the macromolecule [19], so $I(0) \sim c_0 M$. In the case of macromolecules which behave as mass fractal clusters with characteristic length ξ and mass fractal dimension $D = 2$, as is the case of the present system, the molecular weight scales as $M \sim \xi^2$ [18]. Since the number of macromolecules or clusters in the volume V of the sample should be $N = c_0 V/M$, then the number of macromolecules

or clusters per unit volume of the sample $N_C = N/V$ should be

$$N_C \sim I(0)/\xi^4. \quad (4)$$

Figure 4 shows the evolution of N_C as determined from the ratio $I(0)/\xi^4$.

4. Discussion

The lack of an upturn in the curves of the Zimm plots (figure 2) at high q is typical of polydisperse coils of linear chains or random f -functional branched polycondensates [15]. The evolution of the plots in figure 2 at small q is in perfect analogy with the predictions of the Ornstein–Zernike theory of critical phenomena as temperature approaches the critical point [14]. There is a correlation between the time evolution of the (irreversible) gelling system and the equilibrium temperature as the critical point is approached in the phase transitions associated with critical phenomena. In this case, the correlation function $\gamma(r)$ of the structure is given by $\gamma(r) \sim (1/R^2)(1/r) \exp(-r/\xi)$ [14].

The lack of a maximum in the Kratky plots (figure 3—bottom) is also typical of random polycondensates, but the scattering from random branched polycondensates is indistinguishable from that of the most probable distribution of polydisperse coils of linear chains [15]. The functionality f of the branching units seems to be less than 3 for the lack of a maximum in the Kratky plots [15].

The constancy of Q along the gelling process in the system studied here suggests an aggregation process by a phase separation by coarsening. The power law $\xi \sim t^1$ growth of the clusters found after an initial period suggests a mechanism of growth which is more rapid than the typical $\xi \sim t^{1/3}$ or $\xi \sim t^{1/2}$ for pure diffusion controlled cluster–cluster aggregation mechanisms. It has been pointed out that physical forces (hydrothermal forces) should be actuating together with diffusion in the gelling process of this system [6, 8]. This could be the case of the gelling system studied here. However, the lack of a maximum in the curves $I(q)$ does not support a mechanism of phase separation by spinodal decomposition.

The evolution of the number of clusters N_C per unit volume of the sample in absolute cm^{-3} units could be estimated with good approximation for the present system from the knowledge of the characteristic length a of the primary particle and of the volume fraction ϕ of the silica particles. If m_0 is the mass of the primary particle building up the mass fractal cluster with molecular weight M and characteristic length ξ , then $M = m_0(\xi/a)^D$ [20], or simply $M = m_0(\xi/a)^2$ for the case of the present system with $D = 2$. Since $c_0 V = n_0 m_0$ and $\phi = n_0 a^3/V$, where n_0 is the number of primary silica particles in the volume V of the sample, then $N_C = c_0/M$ could be cast with good approximation by

$$N_C = (\phi/a)\xi^{-2}. \quad (5)$$

There is no crossover at high- q in the SAXS curves (figure 1) accounting for the characteristic size a of the primary silica particle. So, a should be smaller than the experimental $1/q_m \sim 0.23$ nm. As a conservative position, we assumed

$a \sim 1/q_m \sim 0.23$ nm in order to express N_C in absolute cm^{-3} units in figure 4. Equations (4) and (5) are in good agreement with the experimental $I(0)$ and ξ .

5. Conclusions

The structural evolution of the gelling silica sols, prepared by a two-step acid–base process of TEOS sonohydrolysis, can be described by the evolution of a correlation function given approximately by $\gamma(r) \sim (1/R^2)(1/r) \exp(-r/\xi)$, where ξ is the structure correlation length and R is a chain persistence length. The characteristic length ξ grows following approximately a power law with time t as $\xi \sim t^1$, after an initial period in which the growth of ξ is slower, while R remains undetermined but has a practically constant value with time, except for a small relative increase of about 15% in the initial period.

The characteristics of the scattering from the gelling system are typical of systems built up by polydisperse coils of linear chains or branched polycondensates of random f -functional units, but the scattering from random branched polycondensates is indistinguishable from that of the most probable distribution of polydisperse coils of linear chains.

The structural evolution with time is compatible with an aggregation process by a phase separation by coarsening. The mechanism of growth seems to be more rapid than others typically observed for pure diffusion controlled cluster–cluster aggregation mechanisms. This suggests that physical forces (hydrothermal forces) could be actuating together with diffusion in the gelling process of this system. However, the data apparently do not support a spinodal decomposition mechanism, at least starting from the stable acid sol studied here.

Acknowledgments

This research was partially supported by LNLS—National Synchrotron Light Laboratory, FAPESP and CNPq.

References

- [1] Schaefer D W and Keefer K D 1984 *Phys. Rev. Lett.* **53** 1383
- [2] Lours T, Zarzycki J, Craievich A, dos Santos D I and Aegerter M 1988 *J. Non-Cryst. Solids* **100** 207
- [3] Blanco E, Ramírez-del-Solar M, de la Rosa-Fox N and Craievich A F 1992 *J. Non-Cryst. Solids* **147/148** 238
- [4] Šefčík J and McCormick A V 1997 *Catal. Today* **35** 205
- [5] Vollet D R, Donatti D A and Ibañez Ruiz A 2001 *J. Non-Cryst. Solids* **288** 81
- [6] Gommès C, Blacher S, Goderis B, Pirard R, Heinrichs B, Alié C and Pirard J P 2004 *J. Phys. Chem. B* **108** 8983
- [7] Ratajska-Godomaska B and Gadomski W 2004 *J. Phys.: Condens. Matter* **16** 9191
- [8] Gommès C J, Goderis B, Pirard J P and Blacher S 2007 *J. Non-Cryst. Solids* **353** 2495
- [9] Abete T, de Candia A, Lairez D and Coniglio A 2004 *Phys. Rev. Lett.* **93** 228301
- [10] Martin J E and Keefer K D 1986 *Phys. Rev. A* **34** 4988
- [11] Martin J E, Wilcoxon J and Adolf D 1987 *Phys. Rev. A* **36** 1803
- [12] Tordjeman P, Fargette C and Mutin P H 2001 *J. Rheol.* **45** 995
- [13] Botet R and Płoszajczak M 1999 *J. Sol–Gel Sci. Technol.* **15** 167
- [14] Stanley H E 1971 *Introduction to Phase Transition and Critical Phenomena* (Oxford: Science Publications) p 104
- [15] Burchard W 1977 *Macromolecules* **10** 919
- [16] Donatti D A, Ibañez Ruiz A and Vollet D R 2002 *Ultrason. Sonochem.* **9** 133
- [17] Debye P 1947 *J. Phys. Colloid Chem.* **51** 18
- [18] Riello P, Minesso A, Craievich A and Benedetti A 2003 *J. Phys. Chem. B* **107** 3390
- [19] Glatter O and Kratky O 1982 *Small Angle X-ray Scattering* (London: Academic)
- [20] Zarzycki J 1990 *J. Non-Cryst. Solids* **121** 110